Supporting Information

Broadband emission from zero-dimensional Cs_4PbI_6 perovskite nanocrystals

Saikat Bhaumik,*[a,b] Annalisa Bruno,[a] and Subodh Mhaisalkar [a,c]

Experimental details

Materials: Lead oxide (PbO; 99.999 %, trace metals basis), cesium carbonate (Cs_2CO_3; 99.995 %, trace metals basis), tetrabutylammonium iodide (TBAI; 98 %), oleic acid (OA; 90 %), oleylamine (OAm; 70 %), 1-octadecene (ODE; 90 %), toluene (anhydrous, 99.7 %) were purchased from Sigma-Aldrich. All these chemicals were used without further purification.

Preparation of Cs-oleate precursor: Cs_2CO_3 (2.5 mmol, 814 mg) was mixed with OA (2.5 mL) and ODE (40 mL) in a 100 mL three-necked round-bottom glass flask.[1] At first, the mixed solution was dried under vacuum for one hour at 120 ℃. Then the reaction mixture was heated under a flow of N_2 for another hour at 150 ℃ until all Cs_2CO_3 reacted with OA and a transparent solution was obtained. Before injection during synthesis, the Cs-oleate precursor was preheated to 100 ℃.

Preparation of TBAI precursor: TBAI (2 mmol) was mixed in OAm (7 mL) and ODE (3 mL) in a 100 mL round-bottom flask.[1] The mixture was kept under vacuum for one and half hours at 150 ℃ and was subsequently heated at 200 ℃ for one hour under an N_2 atmosphere. The appearance of the final solution was pale yellow.

Synthesis of Cs_4PbI_6 NCs: In the first step, PbO (0.2 mmol, 45 mg), OAm (0.2 mL), OA (1 mL), and ODE (3 mL) were mixed in a round-bottom flask. The mixture was dried under vacuum for 1.5 hours at 100℃, after which the temperature was lowered to 80 ℃ under a flow of N_2 for an additional hour. After complete dissolution of PbO, the reaction temperature was increased to the desired temperature (100 ℃-180 ℃), and TBAI precursor (2 mL) was swiftly injected. After ten minutes, *Cs*-oleate precursor (0.4 mL) was injected into the reaction mixture. The reaction was prolonged for five minutes and then quenched in a cold water bath.

Experimental section

Optical measurement: Excitation-wavelength-dependent PL and PLE spectra were measured with a NanoLog (Horiba Jobin Yvon) using 5 nm entrance and exit slits and 0.5

sec of integration time. In order to study the temperature-dependence properties of our sample, we conducted temperature-dependent PL measurement by combining a heating and freezing microscope stage (Linkam Scientific, THMS 600) into optical measurement systems. The freezing process was realized by cooling the stage with Liquid Nitrogen, and the temperature was controlled by TMS 94 programmer, which has a temperature accuracy of ±0.1 ℃.

TRPL dynamics were measured using a micro-PL system, incorporating a Nikon microscope and a Picoquant PicoHarp 300 time-correlated single photon counting (TCSPC) system. A ps pulsed laser diode was used as excitation source. The output signal was processed through Acton SP-2300i monochromator for spectral selection of the emission light coupled to an avalanche diode synchronized with excitation laser via TCSPC electronic. The full width at half maximum of the system instrument respond function is around 50 ps.

The power dependent PL spectra excited at 2.33 eV and 2.71 eV were measured using a Witec alpha 300 backscattering con-focus Raman system. The laser beam was focused on the sample using an objective (Nikon, 50×/NA0.45) and the size of the laser beam is as small as 600 nm. We used two BragGrate Notch Filters (BNF) centered at 532 nm with bandwidths as narrow as 5 cm^{-1} and a large OD (>4) to achieve low-frequency region. The spectra were dispersed by an 1800 lines/mm grating and detected using a TE-cooled CCD. For power-dependent PLE spectra excited at 2.71 eV, we used an MBL-F-457 Solid State laser. The size of the laser beam was around 500 nm which was also focused on the sample using an objective (Nikon, 50×/NA0.45). The spectra were dispersed by a 150 lines/mm grating and detected using a TE-cooled CCD. For the power-dependent PL spectra excited at 2.33 eV, we used two BragGrate Notch Filters (BNF) centered at 532 nm with bandwidths as narrow as 5 cm^{-1}, so that we could achieve signals very close to laser line. In order to get spectra with a large range, we used a 150 lines/mm grating and detected using a TE-cooled CCD. A series of neutral optical density filters and one continuous neutral optical density filter was used to vary the incident laser power from 1 nW to 10 mW. The laser power was monitored with Thorlabs PM100D laser power meter.

In order to study the temperature-dependence properties of our sample, we conducted temperature-dependent Raman by combining a heating and freezing microscope stage (Linkam Scientific, THMS 600) into optical measurement systems. The freezing process was realized by cooling the stage with Liquid Nitrogen, and the temperature was controlled by TMS 94 programmer, which has a temperature accuracy of ±0.1 ℃.

We suspect that the Cs_4PbI_6 NCs may degrade under normal atmospheric conditions. We have synthesized our NCs via hot-injection colloidal synthetic methods under the nitrogen

atmosphere. We use freshly synthesized Cs_4PbI_6 NCs to prepare the thin-films in the glove box. For low-temperature measurements, we have transfer the nanocrystalline thin-film inside the nitrogen-filled chamber (10^{-3} mbar) and the temperature is controlled electronically controlled by controlling the nitrogen fluxmicroscope stage (Linkam Scientific, THMS 600). For each temperature we have stabilized the desired value for 5 minutes before performing each of absorbance, PL, and other measurements. We have repeated low-temperature PL measurements several times to check the reproducibility. The results have consistently confirmed the white light emission at low temperature and the PL intensity increases with decrease in temperature.

Transmission electron microscope (TEM) Characterization: TEM images were carried out with a JEOL-2010 TEM (JEOL, Tokyo, Japan Cs = 0.5 mm and Cc = 1.1 mm) operated at 200 kV with a LaB_6 source. Synthesized Cs_4PbI_6 nanocrystals were dispersed in toluene and then a drop of suspension was placed on a holey carbon-coated copper grid that was allowed to dry.

Powder X-ray diffraction (PXRD) characterization: The solution of Cs_4PbI_6 nanocrystals drop casted on a glass substrate and dried under vacuum for sample preparation. X-Ray diffraction analysis was carried out with the Bruker D8 Advance system equipped with a Cu K_α X-ray tube operated at 40 kV.

Temperature-dependent absorption spectra:

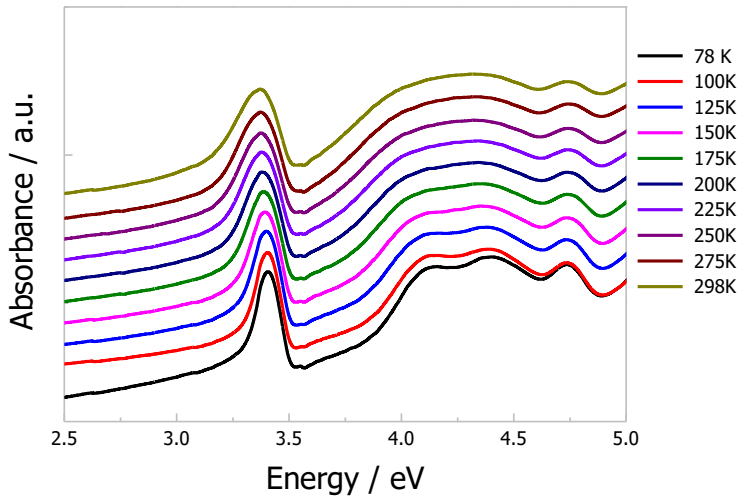

Figure S1. *Temperature-dependent absorbance spectra of Cs_4PbI_6 NCs film from 78 K to 298 K.*

Determination of exciton binding energy: In order to get exciton binding energy of Cs_4PbI_6 NCs, we did Tauc plot of measured absorbance (78 K), as is shown in Figure S1. The strong absorption peak is attributed to the exciton absorption. The red line is the linear fitting of the band edge, its cross-section with the X-axis (black line) is the obtained bandgap for Cs_4PbI_6 NCs. Then we calculated the exciton binding energy to be 490 meV.

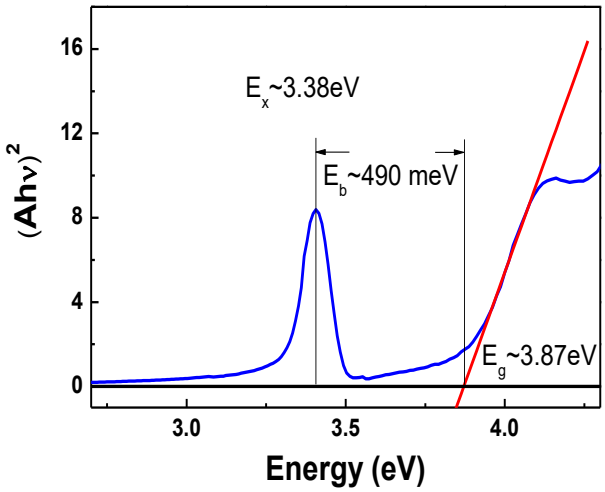

Figure S2. *Tauc plot of the Cs_4PbI_6 NCs film based on its absorption spectra at 78 K.*

Temperature-dependent PL spectra:

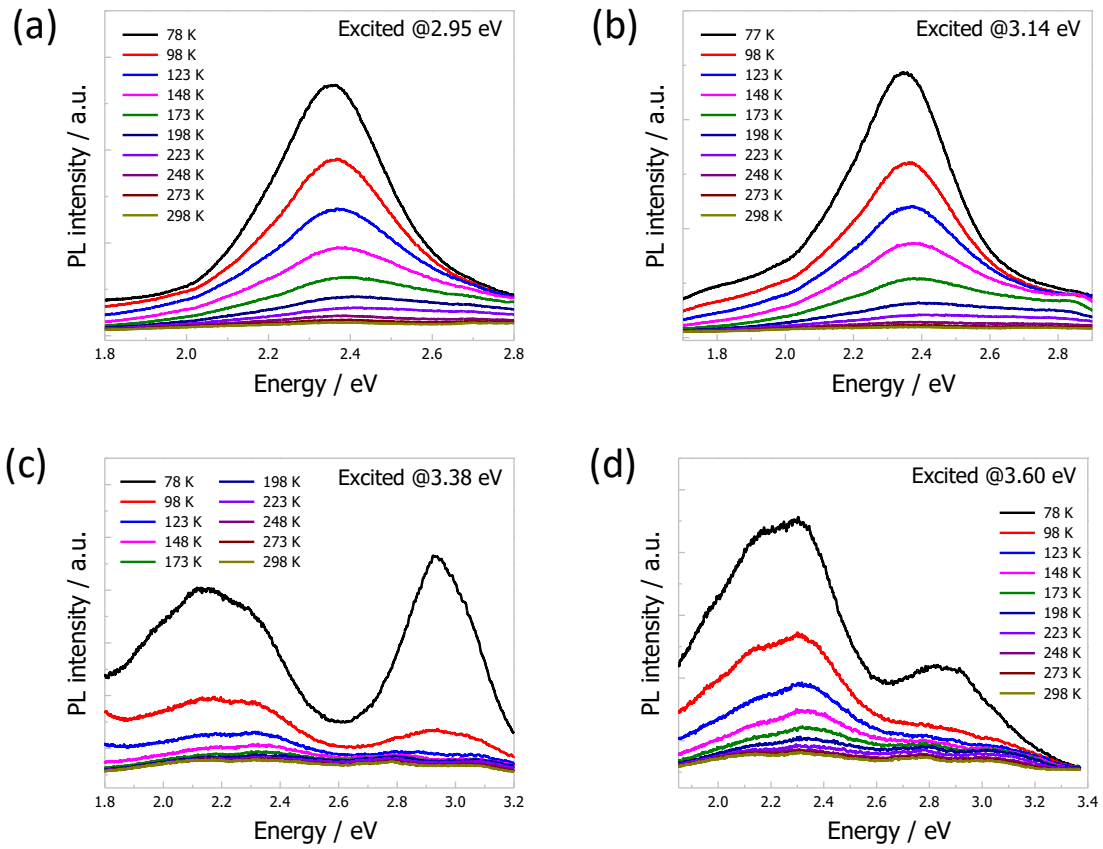

Figure S3. *Temperature-dependent PL spectra of Cs_4PbI_6 NCs film excited at various energies of (a) 2.95 eV, (b) 3.14 eV, (c) 3.38 eV and (d) 3.60 eV. The temperature varied from 78 K to 298 K.*

We conducted temperature-dependent PL measurement with various excitation energies of 3.60, 3.38, 3.14 and 2.95 eV as represented in Figure S3. It is noticeable that with decreasing temperature the emission at around 2.95 eV increased gradually. Figure S3b is the spectra with real intensity. The PL intensity was enhanced around 30 times when cooling the sample from 298 K to 78 K.

White light emission of Cs_4PbI_6 NCs at 78 K:

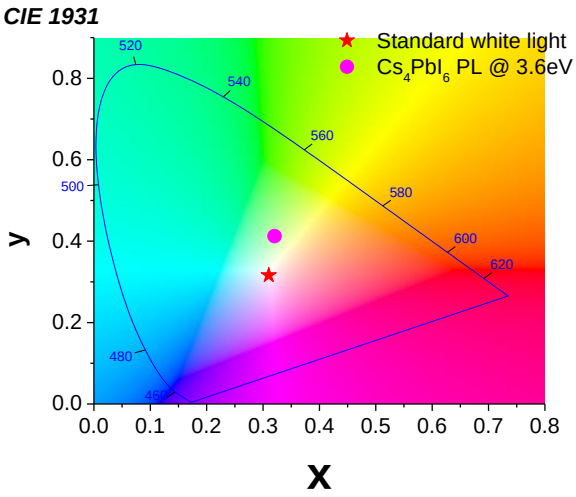

Figure S4. *The CIE 1931 chromaticity map. The pink circle is the position for Cs_4PbI_6 NCs emission spectra observed at 78 K.*

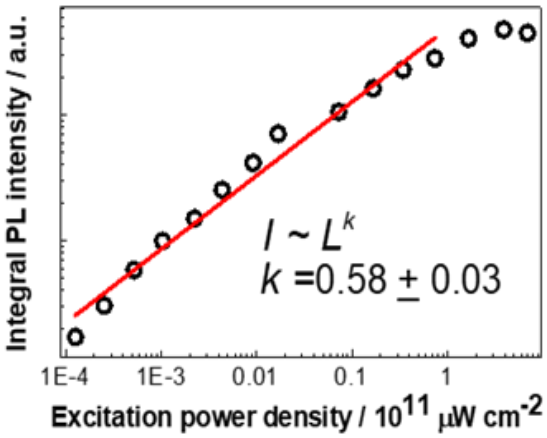

Figure S5. *Integral PL intensity of power-dependent PL spectra of the Cs_4PbI_6 NCs film excited at 2.71 eV at 78 K and the fitting results with the power law.*

Temperature-dependent Raman spectra:

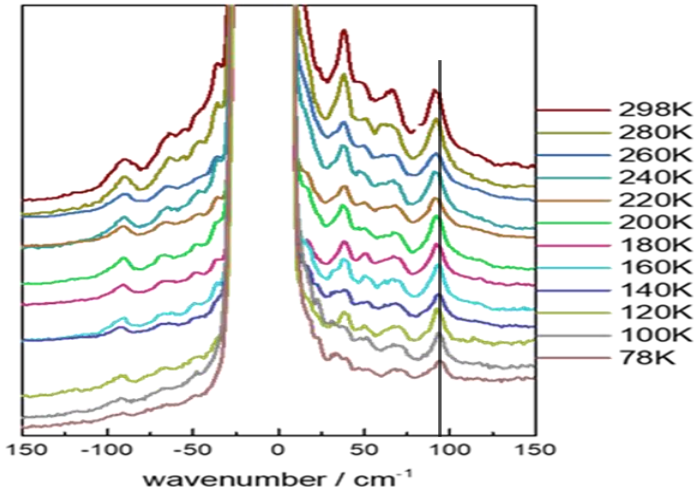

Figure S6. *Temperature-dependent Raman spectra of Cs_4PbI_6 NCs film while the temperature is varied from 78 K to 298 K.*

Temperature-dependent XRD diffraction pattern:

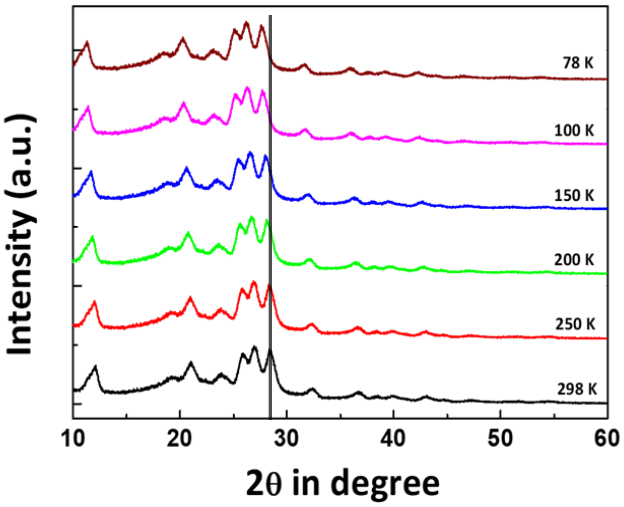

Figure S7. *Temperature-dependent XRD diffraction pattern of Cs_4PbI_6 NCs while the temperature is varied from 78 K to 298 K.*

Time-resolved photoluminescence (TRPL) experiments:

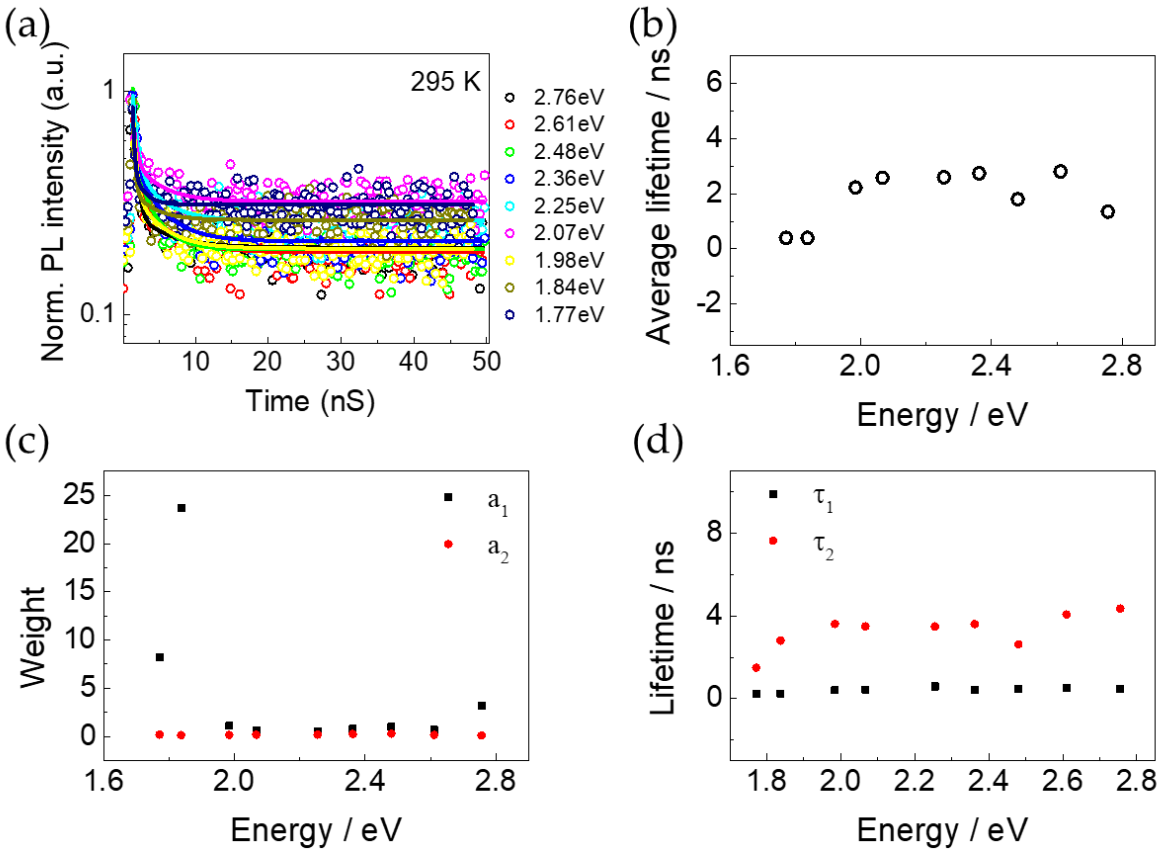

Figure S8. *(a) Normalized TRPL spectra detected at different energy excited at 3.38 eV at 295 K. Open circles are experimental data. Corresponding solid lines are fitting results of a two-exponential function. (b) Average lifetimes at different energy obtained from TRPL results in the left panel. Obtained weight (c) and lifetime (d) at different detecting energy through fitting TRPL spectra with a two-exponential function.*

Table S1. *Fitting results of TRPL spectra at 295K with two-exponential function,* $I(t) = I_0\left[a_1\, exp\left(\frac{t}{\tau_1}\right) + a_2\, exp\left(\frac{t}{\tau_2}\right)\right]$.

Energy (eV)	Wavelength (nm)	a_1	τ_1 (ns)	a_2	τ_2 (ns)	τ_{ave} (ns)
2.75556	450	3.21669	0.45895	0.10091	4.35437	1.35243
2.61053	475	0.67547	0.53311	0.16074	4.06548	2.81052
2.48	500	1.0168	0.45763	0.29262	2.62591	1.8081
2.3619	525	0.80227	0.43409	0.25982	3.60526	2.7458
2.25455	550	0.5167	0.58663	0.19692	3.48661	2.59844
2.06667	600	0.62428	0.44028	0.18354	3.49743	2.58087
1.984	625	1.10476	0.41466	0.16665	3.60967	2.22843
1.83704	675	23.69989	0.2489	0.13042	2.8108	0.39879
1.77143	700	8.21136	0.21688	0.19865	1.49617	0.39985

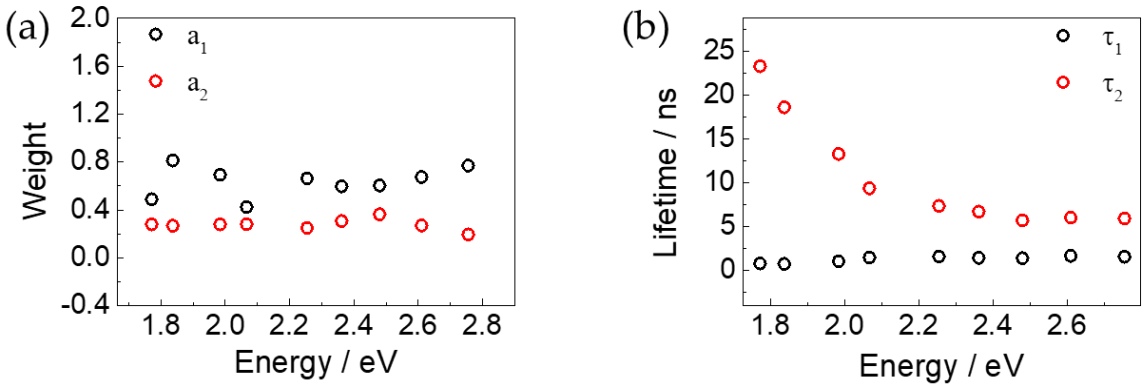

Figure S9. *Obtained weight (a) and lifetime (b) at different detecting energy through the two exponential fitting of TRPL spectra in Figure 5.*

Table S2. *Fitting results of TRPL spectra at 78 K with two-exponential function,* $I(t) = I_0\left[a_1\, exp\left(\frac{t}{\tau_1}\right) + a_2\, exp\left(\frac{t}{\tau_2}\right)\right]$.

Energy (eV)	Wavelength (nm)	a_1	τ_1(ns)	a_2	τ_2(ns)	τ_{ave}(ns)
2.75556	450	0.77037	1.58324	0.1957	5.94935	3.71557
2.61053	475	0.67514	1.67574	0.27098	6.04585	4.26074
2.48	500	0.60455	1.41707	0.36458	5.72063	4.4676
2.3619	525	0.5973	1.44615	0.30733	6.72545	5.16946
2.25455	550	0.66391	1.59709	0.25066	7.38677	5.27854
2.06667	600	0.42467	1.48725	0.28132	9.3872	7.86247
1.984	625	0.6948	1.07407	0.27972	13.30898	11.26594
1.83704	675	0.81345	0.75436	0.2691	18.64382	16.69422
1.77143	700	0.48992	0.82376	0.28011	23.33593	22.02684

References

1 S. Bhaumik; S. A. Veldhuis; S. K. Muduli; M. Li; R. Begum; T. C. Sum; S. Mhaisalkar and N. Mathews, *ChemPlusChem* 2018, **83**, 514.